



Three-Body Amplification of Photon Heat Tunneling Supplementary Material

Riccardo Messina, Mauro Antezza, Philippe Ben-Abdallah

► To cite this version:

Riccardo Messina, Mauro Antezza, Philippe Ben-Abdallah. Three-Body Amplification of Photon Heat Tunneling Supplementary Material. *Physical Review Letters*, 2012, 109 (244302), pp.244302. 10.1103/PhysRevLett.109.244302 . hal-00763953

HAL Id: hal-00763953

<https://hal.science/hal-00763953>

Submitted on 11 Dec 2012

HAL is a multi-disciplinary open access archive for the deposit and dissemination of scientific research documents, whether they are published or not. The documents may come from teaching and research institutions in France or abroad, or from public or private research centers.

L'archive ouverte pluridisciplinaire **HAL**, est destinée au dépôt et à la diffusion de documents scientifiques de niveau recherche, publiés ou non, émanant des établissements d'enseignement et de recherche français ou étrangers, des laboratoires publics ou privés.

Three-Body Amplification of Photon Heat Tunneling Supplementary Material

Riccardo Messina,¹ Mauro Antezza,^{2,3} and Philippe Ben-Abdallah¹

¹*Laboratoire Charles Fabry, UMR 8501, Institut d'Optique, CNRS,
Université Paris-Sud 11, 2 Avenue Augustin Fresnel, 91127 Palaiseau Cedex, France.*

²*Laboratoire Charles Coulomb UMR 5221, Université Montpellier 2, F-34095 Montpellier, France*

³*Laboratoire Charles Coulomb UMR 5221, CNRS, F-34095 Montpellier, France*

We give in the following some technical details concerning the calculation presented in the paper. In particular, we address the precise definition of the reflection and transmission operators describing the three slabs, we discuss the calculation of the temperature T_2 of the intermediate body, and consider the transmission probabilities in the (ω, k) plane.

I. REFLECTION AND TRANSMISSION COEFFICIENTS

In the planar geometry considered, the three bodies are described in terms of their reflection and transmission coefficients: these are functions of the thicknesses of the slabs and of their material properties. In particular, the quantities $\rho_{ip}(\mathbf{k}, \omega)$ and $\tau_{ip}(\mathbf{k}, \omega)$ associated to a given slab $i = 1, 2, 3$ (appearing in eqs. (3), (5) and (6) of the paper) are defined as

$$\rho_p(\omega, \mathbf{k}) = r_p(\omega, \mathbf{k}) \frac{1 - e^{2ik_{zm}\delta}}{1 - r_p^2(\omega, \mathbf{k})e^{2ik_{zm}\delta}}, \quad \tau_p(\omega, \mathbf{k}) = \frac{t_p(\omega, \mathbf{k})\bar{t}_p(\omega, \mathbf{k})e^{ik_{zm}\delta}}{1 - r_p^2(\omega, \mathbf{k})e^{2ik_{zm}\delta}}. \quad (1)$$

In the paper, we have defined $\delta = \delta_2$ (see Fig. 1 of the paper). In these definitions we have introduced the z component of the wavevector inside the medium,

$$k_{zm} = \sqrt{\varepsilon(\omega) \frac{\omega^2}{c^2} - \mathbf{k}^2}, \quad (2)$$

$\varepsilon(\omega)$ being the complex dielectric permittivity of the slab, the ordinary vacuum-medium Fresnel reflection coefficients

$$r_{\text{TE}} = \frac{k_z - k_{zm}}{k_z + k_{zm}}, \quad r_{\text{TM}} = \frac{\varepsilon(\omega)k_z - k_{zm}}{\varepsilon(\omega)k_z + k_{zm}}, \quad (3)$$

as well as both the vacuum-medium (noted with t) and medium-vacuum (noted with \bar{t}) transmission coefficients

$$\begin{aligned} t_{\text{TE}} &= \frac{2k_z}{k_z + k_{zm}}, & t_{\text{TM}} &= \frac{2\sqrt{\varepsilon(\omega)}k_z}{\varepsilon(\omega)k_z + k_{zm}}, \\ \bar{t}_{\text{TE}} &= \frac{2k_{zm}}{k_z + k_{zm}}, & \bar{t}_{\text{TM}} &= \frac{2\sqrt{\varepsilon(\omega)}k_{zm}}{\varepsilon(\omega)k_z + k_{zm}}. \end{aligned} \quad (4)$$

We observe that in the limit $\delta \rightarrow +\infty$ of infinitely-thick slab 2 we have $\rho_{2p} \rightarrow r_{2p}$ and $\tau_{2p} \rightarrow 0$. As a consequence, the transmission coefficient $\mathcal{T}_{3s,p}^{(12)}$ (see eq. (5) of the paper) vanishes and we recover the ordinary expression of the heat transfer between two slabs (slabs 2 and 3 in this case). In absence of slab 1 ($\rho_{1p} \rightarrow 0$) we obtain again $\mathcal{T}_{3s,p}^{(12)} \rightarrow 0$ and $\rho_{12p} \rightarrow \rho_{2p}$ so that the two-slab expression is recovered.

II. TEMPERATURE OF THE INTERMEDIATE SLAB

The geometrical configuration we have chosen for our calculation is symmetric with respect to the exchange of slabs 1 and 3. This is true both because they are identical (same material and thickness) and because the distance between slabs 1 and 2 coincides with the one between slabs 2 and 3 (equal to d in both cases). As a consequence, we have $\rho_{1p} = \rho_{3p}$ and moreover the transmission probabilities $\mathcal{T}_{3s,p}^{(12)}$ and $\mathcal{T}_{3s,p}^{(23)}$ (eq. (5) of the paper) are also independent of the exchange $1 \leftrightarrow 3$. In order to express the heat flux on body 1 we can thus simply exchange 1 and 3 in the

Boltzmann populations $n_{12}(\omega)$ and $n_{23}(\omega)$ in eq. (4) of the paper. Since we are dealing with the (evanescent) heat exchanged between the bodies, the heat flux on body 2 can be expressed as the opposite of the sum of the heat fluxes on bodies 1 and 3. We then have

$$\begin{aligned}\phi_{3s}(\omega, d, \delta) &= -\hbar\omega \sum_p \int_{ck>\omega} \frac{d^2\mathbf{k}}{(2\pi)^2} \left[\left(n_{12}(\omega) + n_{32}(\omega) \right) \mathcal{T}_{3s,p}^{(12)}(\omega, \mathbf{k}, d, \delta) + \left(n_{23}(\omega) + n_{21}(\omega) \right) \mathcal{T}_{3s,p}^{(23)}(\omega, \mathbf{k}, d, \delta) \right] \\ &= \hbar\omega \left(2n(\omega, T_2) - n(\omega, T_1) - n(\omega, T_3) \right) \sum_p \int_{ck>\omega} \frac{d^2\mathbf{k}}{(2\pi)^2} \left[\mathcal{T}_{3s,p}^{(12)}(\omega, \mathbf{k}, d, \delta) - \mathcal{T}_{3s,p}^{(23)}(\omega, \mathbf{k}, d, \delta) \right].\end{aligned}\quad (5)$$

We thus see that the geometrical and material properties contained in the difference of transmission probabilities are weighted over the overall temperature-dependent factor $2n(\omega, T_2) - n(\omega, T_1) - n(\omega, T_3)$. As we see from Fig. 3 of the paper, the assumption of quasi-monochromatic heat-flux spectrum at $\omega = \omega_{\text{spp}}$ is reasonably accurate. As a consequence, in order to make the flux on body 2 vanish, eq. (5) allows us to provide a very simple condition to estimate the temperature T_2 : this temperature is the solution of the equation

$$2n(\omega_{\text{spp}}, T_2) - n(\omega_{\text{spp}}, T_1) - n(\omega_{\text{spp}}, T_3) = 0, \quad (6)$$

which gives

$$T_2 = \frac{\hbar\omega_{\text{spp}}}{k_B} \left[\log \left(1 + \frac{2}{n(\omega_{\text{spp}}, T_1) + n(\omega_{\text{spp}}, T_3)} \right) \right]^{-1}. \quad (7)$$

We have verified that the numerically-calculated temperature T_2 and the estimate given by eq. (7) differ at most by 2%.

III. MODES OF THE THREE-SLAB SYSTEM

We discuss here the dependence of the two- and three-body transmission probabilities defined in eqs. (3) and (5) of the paper on the ω and k , for a given couple (d, δ) . In accordance with the discussion given in the paper, we will compare \mathcal{T}_{2s} with $\mathcal{T}_{3s} = (\mathcal{T}_{3s}^{(12)} + \mathcal{T}_{3s}^{(23)})/2$. These two quantities are plotted in Fig. 1 in the (ω, k) plane for $d = 700$ nm and the associated optimal value of the thickness $\delta = 870$ nm.

As a first observation, we see that the resonant peak in the spectral flux plotted in Fig. (3) of the paper is due to the presence of a resonant surface modes which exist only in TM polarization. Moreover we note that, while in the two-body case we have one symmetric and one antisymmetric mode [1], we observe the appearance of two supplementary modes in presence of an intermediate slab which results from doubling the number of cavities (and interfaces) in the system. Moreover, as clearly shown in Fig. 1, in the three-slab case these modes remain efficient up to larger values of k . These features result in the enhancement and broadening of the resonance peak of the spectral flux. For both polarizations, the presence of supplementary (frustrated) modes at low frequencies explains the secondary peak in the spectral flux in Fig. 3 of the paper. The number and efficiency of those modes is reduced in the three-body configuration: this explains why the amplification mechanism is centered around the resonance frequency of both surface modes.

[1] E. N. Economou, Phys. Rev. **182**, 539 (1969).

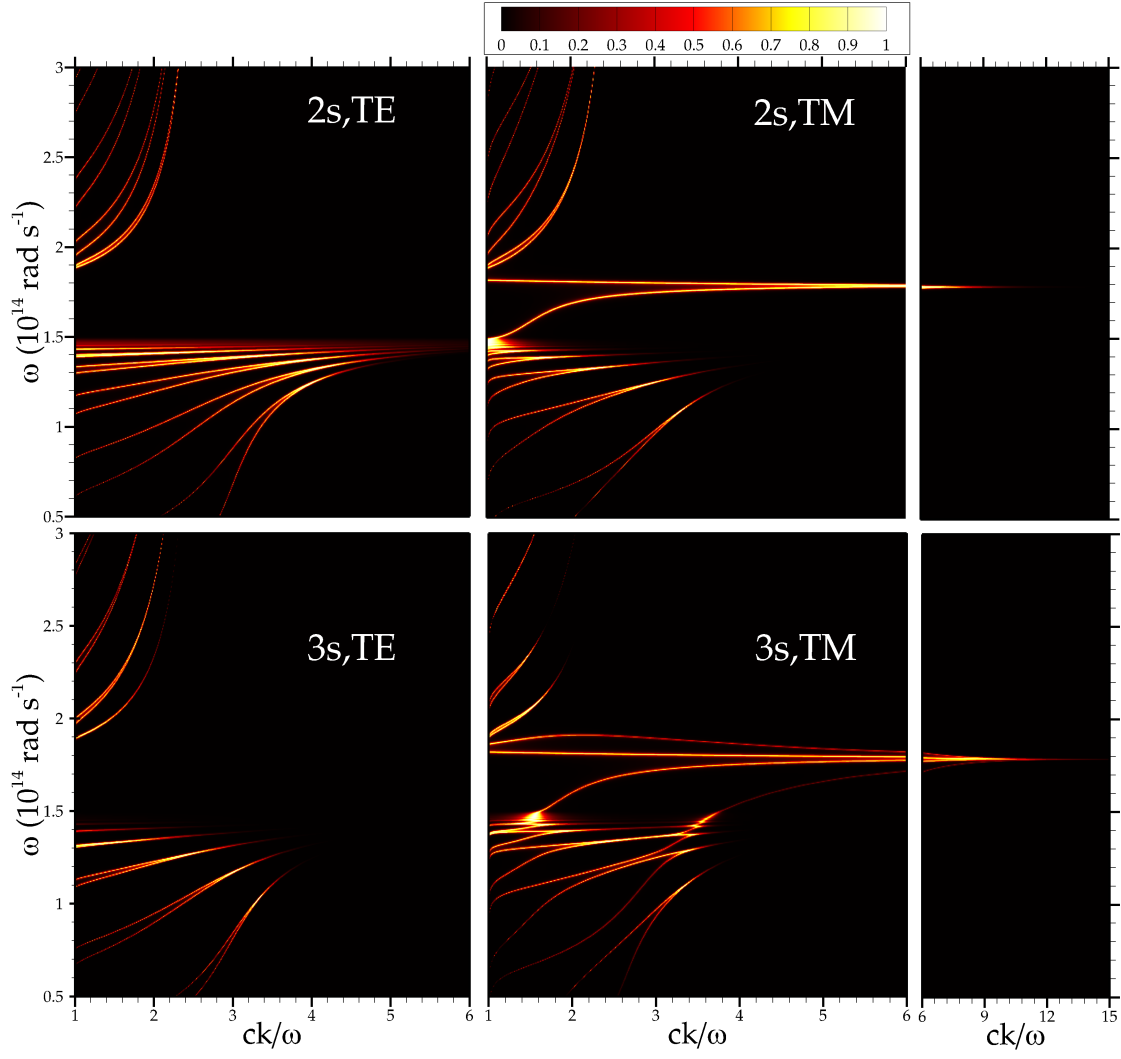


FIG. 1: Two- (upper side) and three-body (lower side) transmission probabilities for both polarizations as a function of ω and k at separation distance $d = 700 \text{ nm}$ and $\delta = 870 \text{ nm}$.